Intermediate-Temperature Operation of Sodium Secondary Batteries with High Rate Capability and Cyclability Using Ionic Liquid Electrolyte

K. Matsumoto[a], C. Y. Chen[a], T. Kiko[a], J. Hwang[a], T. Hosokawa[a], T. Nohira[b], and R. Hagiwara[a]

[a] Graduate School of Energy Science, Kyoto University, Yoshida, Kyoto 606-8501, JAPAN
[b] Institute of Advanced Energy, Kyoto University, Gokasho, Uji 611-0011, JAPAN

Electrochemical behavior of Na metal is one of the key factors to construct high performance Na secondary batteries. The present study reports temperature dependence of Na metal deposition/dissolution efficiency and morphology of the deposited Na metal in the Na[FSA]-[C$_2$C$_1$im][FSA] ionic liquids (C$_2$C$_1$im$^+$ = 1-ethyl-3-methylimidazolium and FSA$^-$ = bis(fluorosulfonyl)amide). The deposition/dissolution efficiency shows the minimum at 298 K and increases by both increasing and decreasing temperature. Optical microscopic analysis reveals that Na metal is grown in a whisker-like form during cathodic polarization at 298 K, whereas smooth deposits are observed at 363 K. Although the deposition form at 273 K is also whisker-like, the thickness and length of each whisker is smaller and shorter, respectively, than those at 298 K. Such differences in morphology affect the Na metal deposition/dissolution efficiencies.

Introduction

Ionic liquid electrolytes are widely studied to construct safe electrochemical devices owing to their unique properties such as low volatility, low flammability, and wide liquid-phase temperature range (1), which includes the case of Na secondary batteries which are expected as an alternative energy storage device near future (2-5). Ionic liquids based on sulfonylamide anions (bis(fluorosulfonyl)amide anion (FSA$^-$)) are attractive as electrolytes owing to their low melting point, low viscosity, and high ionic conductivity as well as high stability against cathodic reactions (6-8). Our previous works revealed that FSA-based ionic liquid electrolytes show appealing properties for Na secondary batteries from room temperature to intermediate temperature (4, 5). In particular, intermediate-temperature operation of Na secondary batteries is quite attractive to enhance their performance using waste heat or self-heating of the batteries, and a variety of positive and negative electrodes show good performance in this system (9-12).

Steady utilization of a Na metal negative electrode is one of the key technologies to realize a high-rate and long-life Na secondary batteries. It was reported that Na metal can be reversibly deposited and dissolved in the Na[FSA]-[C$_2$C$_1$im][FSA] (C$_2$C$_1$im$^+$ = 1-ethyl-3-methylimidazolium and FSA$^-$ = bis(fluorosulfonyl)amide) ionic liquid electrolyte (4). This is based on the formation of stable surface film on the Na metal according to the recent works (13, 14). The present study reports temperature dependence of

deposition/dissolution efficiency and morphology of Na metal in the Na[FSA]-[C$_2$C$_1$im][FSA] ionic liquid system.

Experimental

<u>Materials</u>

Air sensitive materials were handled in a glovebox under a dried and deoxygenated argon atmosphere. Volatiles were handled in a vacuum line made of stainless steel. The Na[FSA]-[C$_2$C$_1$im][FSA] (30:70 in molar ratio) ionic liquid was prepared by mixing dry Na[FSA] and [C$_2$C$_1$im][FSA].

<u>Analysis</u>

Electrochemical measurements were performed with a Hokuto Denko charge-discharge system (HJ1001SD8). The Na deposition/dissolution test was performed in a two-electrode cell at a current density of 1.0 mA cm^{-2} using a Hokuto HJ1001SD8 system. Sodium metal of 0.8 C cm^{-2} was first deposited on a Cu substrate and Na deposition and dissolution of 0.2 C cm^{-2} were repeated until the electrode potential reached 0.5 V vs. Na$^+$/Na during the dissolution. The average cycle efficiency of Na deposition/dissolution (ε_{cycle}) is obtained according to the following equation (Equation 1) (4, 15):

$$\varepsilon_{cycle} = N_{eff} \cdot Q_{cycle} / (Q_{ex} + N_{eff} \cdot Q_{cycle}) \tag{1}$$

where N_{eff} is cycle number until the electrode potential reached 1.0 V vs. Na/Na$^+$, Q_{cycle} is the electric charge for Na deposition/dissolution for one cycle (0.02 C cm^{-2}), and Q_{ex} is the extra amount of electricity deposited prior to the cycling (0.08 C cm^{-2}). A sodium metal counter electrode was used for this test.

Morphology of Na metal electrodes was visually confirmed by using a two-electrode beaker cell. In each cycle, deposition and dissolution of Na metal was performed at a current density of 0.2 mA cm^{-2} for 1000 s. This cycle was continued 50 times. Deposited Na metal was observed by optical microscopy. Alternatively, an *in situ* optical microscopy was used to evaluate the morphology at the initial state. Deposition of Na metal was performed 5 mA cm^{-2} for 200 s

Results and discussion
<u>Temperature dependence of cycle efficiency for Na metal deposition/dissolution</u>

Table I summarizes cycle efficiency (η_{eff}) for Na metal deposition/dissolution in Na[FSA]-[C$_2$C$_1$im][FSA] (30:70 in molar ratio) at different temperatures. Figure 1 shows the result of deposition/dissolution test at 298 K. The η_{eff} value at 298 K is 64 % as the potential reaches 1.0 V vs. Na$^+$/Na at the 7th cycle. At 363 K, η_{eff} is highly improved to 97 % reaching 152 cycles. This behavior agrees with a previous work (4) and suggests that η_{eff} is not reduced by the reaction of Na metal with the ionic liquid because such a reaction is usually accelerated by the elevation of temperatures.

It is should be noted that η_{eff} is also improved by decreasing temperature (82 % after 18 cycles), which suggests that there could be more than two factors affecting the η_{eff} values.

TABLE I. Summary of Na metal deposition/dissolution cycle tests in Na[FSA]–[C2C1im][FSA] (30:70)

Temperature / K	Cycle number	Cycle efficiency (η_{eff}) / %
273	18	82
283	1	73
298	7	64
323	16	80
343	49	92
353	55	93
363	152	97
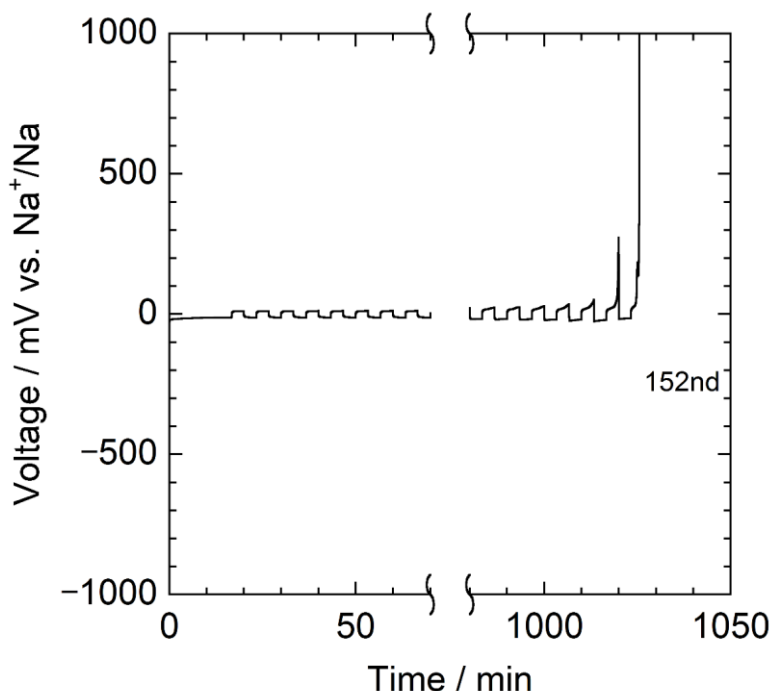
Figure 1. Voltage profiles during the Na deposition/dissolution tests on a Cu plate electrode in Na[FSA]–[C_2C_1im][FSA] (30:70) at 363 K. Current density: 1.0 mA cm^{-2}.

Temperature dependence of morphology of the deposited Na metal

Figure 2 shows the appearance of Na electrodes after alternate Na metal deposition/dissolution for 50 cycles. These electrochemical tests were performed in a two-electrode beaker cell at 273, 298, and 363 K. The appearance of the electrodes apparently changes after 50 cycles. The surface of the Na electrodes is covered with voluminous but sparsely deposited Na metal at 298 K. Although the deposited Na metal at 273 K is slightly denser than that at 298 K, it is still quite fluffy. In the case of the electrode at 363 K, no change is observed and metallic luster is preserved even after 50 cycles.
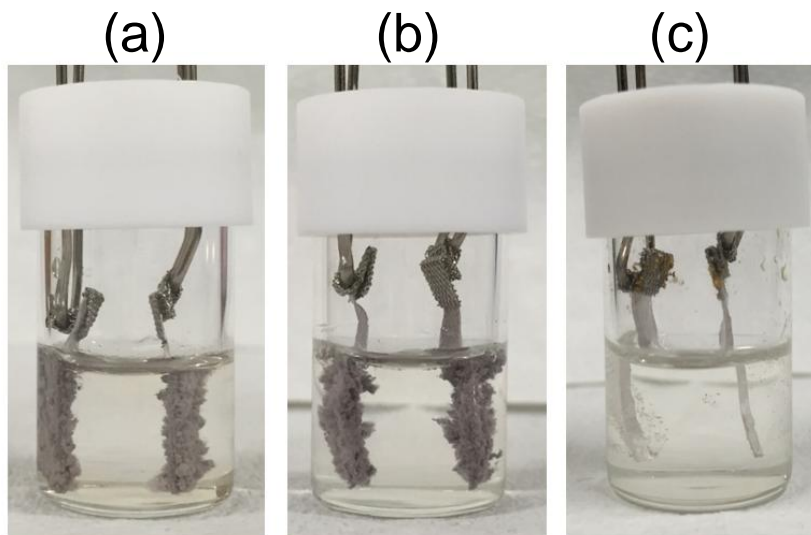
Figure 2. Appearance of the deposited Na metal in Na[FSA]–[C_2C_1im][FSA] (30:70) at (a) 273 K, (b) 298 K, and (c) 363 K. Current density: 0.2 mA cm^{-2}.

The deposits at 273 and 298 K were further examined by optical microscopic analysis as shown in Figure 3. In both the cases, whisker-like deposits with a diameter of a few μm are complicatedly tangled each other. Although some of them have a dendritic form, they are one-dimensionally grown with some bending points in most cases. By carefully looking at the images, one can notice that the deposits at 298 K are thicker in diameter than the one at 273 K. These observations suggest that the morphology of the deposits is highly dependent on the temperature and formation of whisker-like Na metal increases the amount of dead sodium during deposition, leading to the low η_{eff} value.

Morphology during the initial deposition of Na metal on a Cu plate was observed using an *in situ* optical microscopic system. This system is close to the two-electrode coin cell used to estimate η_{eff}. Figure 4 shows optical images of the Na metal deposits at 273, 298, and 363 K. These deposits were obtained by cathodic polarization at a constant current density of 5 mA cm^{-2} for 200 s. For the cathodic polarization at 298 K, nucleation points were relatively sparse at the beginning, and whisker-like Na metal was grown perpendicular to the substrate. After the polarization (Figure 4 (a)), the surface of the substrate is covered with the deposits but the surface of the Cu substrate is still observable. Two-dimensional depth profile analysis revealed that the surface of the deposits is significantly rough and the highest whisker is grown up to 77 μm from the surface of the Cu substrate. At 273 K, nucleation occurs more densely than that at 298 K at the initial stage of cathodic polarization. Although the growth of the deposits obtained after polarization at 273 K is also uneven (Figure (b)), long whisker is not observed and the difference in height is not greater than 8 μm. These results indicate that nucleation is more predominant than nuclear growth at 273 K, which causes the difference in the η_{eff} values at 273 and 298 K. Nucleation at 363 K was not very dense and the deposits were grown in a hemispherical shape with the height of a few μm (Figure 4 (c)). Formation of such dense and smooth deposits leads to the high η_{eff} value at 363 K.
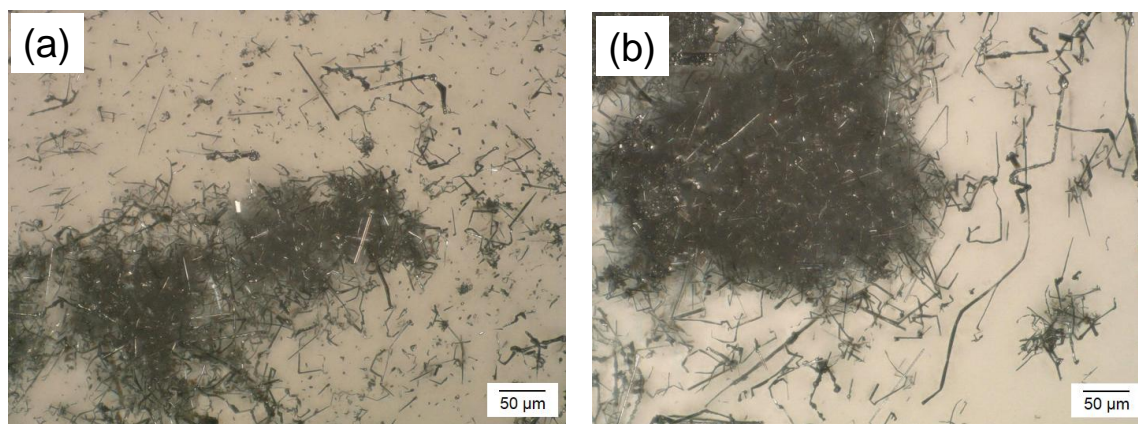
Figure 3. Optical microscopic images of Na metal deposited on Na metal electrodes in Na[FSA]–[C$_2$C$_1$im][FSA] (30:70) at (a) 273 K and (b) 298 K.
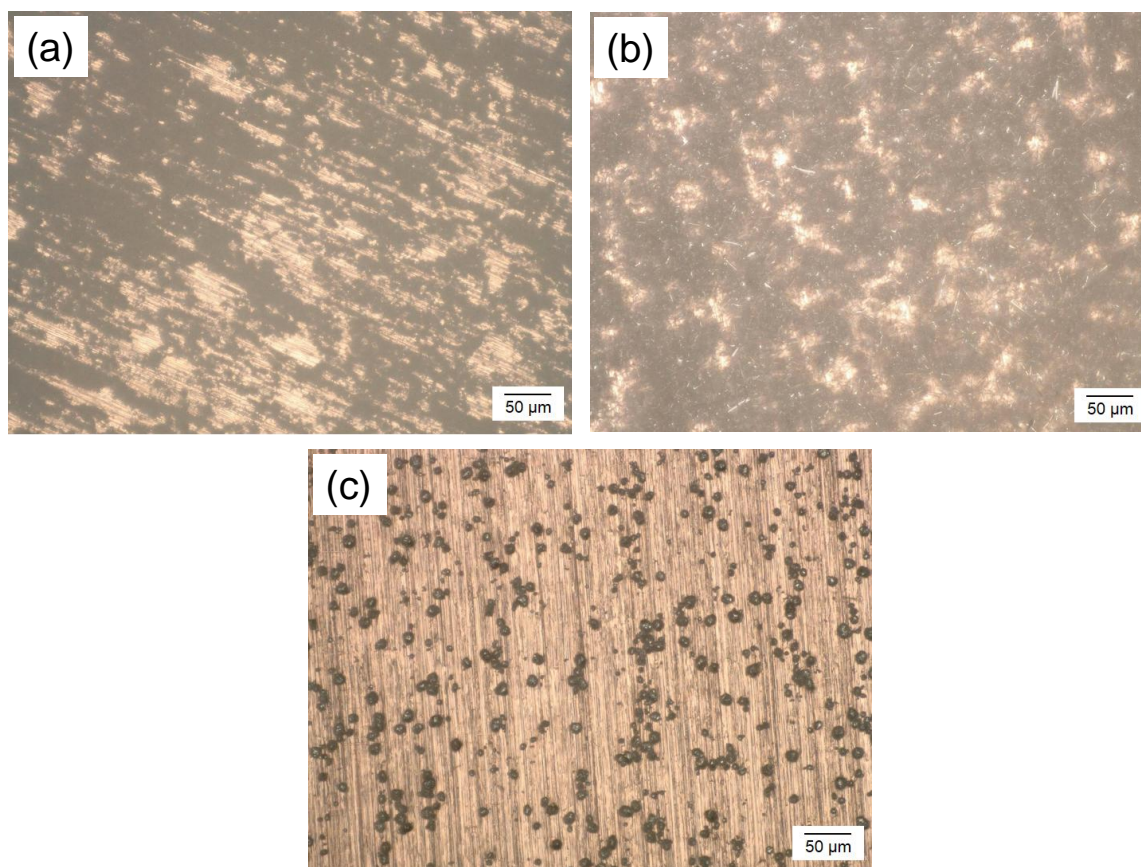

Figure 4 Optical images of deposited Na metal on a Cu plate electrode in Na[FSA]–[C$_2$C$_1$im][FSA] (30:70) at (a) 273, (b) 298, and (c) 363 K. Current density: at 5 mA cm^{-2}. Quantity of electricity: 1.0 C cm^{-2}.

Conclusions

In this study, temperature dependence of Na metal deposition/dissolution efficiency and morphology of the deposited Na metal was investigated in the Na[FSA]-[C$_2$C$_1$im][FSA] ionic liquids. The deposition/dissolution efficiency had the minimum at 298 K and increased at both lower and higher temperatures. The shape of the deposited Na metal was whisker-like at 298 K and spherical at 363 K. The deposition form at 273 K was also whisker-like, each whisker having smaller thickness and shorter length than those at 298 K. Such differences in morphology is considered to affect the Na metal deposition/dissolution efficiencies.

Acknowledgments

References

1. H. Ohno, *Electrochemical Aspects of Ionic Liquids,* John Wiley & Sons Inc., Hoboken, New Jersey, 2011.
2. S. A. M. Noor, P. C. Howlett, D. R. MacFarlane, and M. Forsyth, *Electrochim. Acta*, **114**, 766 (2013).
3. D. Monti, E. Jonsson, M. R. Palacin, and P. Johansson, *J. Power Sources*, **245**, 630 (2014).
4. K. Matsumoto, T. Hosokawa, T. Nohira, R. Hagiwara, A. Fukunaga, K. Numata, E. Itani, S. Sakai, K. Nitta, and S. Inazawa, *J. Power Sources*, **265**, 36 (2014).
5. K. Matsumoto, Y. Okamoto, T. Nohira, and R. Hagiwara, *J. Phys. Chem. C*, **119**, 7648 (2015).
6. M. Ishikawa, T. Sugimoto, M. Kikuta, E. Ishiko, and M. Kono, *J. Power Sources*, **162**, 658 (2006).
7. H. Matsumoto, H. Sakaebe, K. Tatsumi, M. Kikuta, E. Ishiko, and M. Kono, *J. Power Sources*, **160**, 1308 (2006).
8. H. Zhang, W. F. Feng, J. Nie, and Z. B. Zhou, *J. Fluorine Chem.*, **174**, 49 (2015).
9. T. Yamamoto, T. Nohira, R. Hagiwara, A. Fukunaga, S. Sakai, K. Nitta, and S. Inazawa, *J. Power Sources*, **217**, 479 (2012).
10. C. S. Ding, T. Nohira, R. Hagiwara, K. Matsumoto, Y. Okamoto, A. Fukunaga, S. Sakai, K. Nitta, and S. Inazawa, *J. Power Sources*, **269**, 124 (2014).
11. A. Fukunaga, T. Nohira, R. Hagiwara, K. Numata, E. Itani, S. Sakai, K. Nitta, and S. Inazawa, *J. Power Sources*, **246**, 387 (2014).
12. C. Y. Chen, K. Matsumoto, T. Nohira, C. S. Ding, T. Yamamoto, and R. Hagiwara, *Electrochim. Acta*, **133**, 583 (2014).
13. T. Hosokawa, K. Matsumoto, T. Nohira, R. Hagiwara, A. Fukunaga, S. Sakai, and K. Nitta, *J. Phys. Chem. C*, **120**, 9628 (2016).
14. I. A. Shkrob, T. W. Marin, Y. Zhu, and D. P. Abraham, *J. Phys. Chem. C*, **118**, 19661 (2014).

15. K. Matsumoto, R. Taniki, T. Nohira, and R. Hagiwara, *J. Electrochem. Soc.*, **162**, A1409 (2015).